Velocity Ripple Elimination of AC Permanent Motor by using Internal Model Principle*

Wai-Chuen Gan, Li Qiu
Department of Electrical an Electronic Engineering
The Hong Kong University of Science and Technology, Clear Water Bay, Hong Kong, China
Phone: 852-2358-8539 Fax: 852-2358-1485
Email:{eewcgan,eeqiu}@ee.ust.hk

Abstract- *A general AC PM (Permanent Magnet) motor control system consists of a motion controller, a current tracking amplifier, a feedback encoder and the motor itself. The motion controller generates two analog commands to the current tracking amplifier and the three phase currents are reproduced at the motor terminals. However, DC offsets are always present at the motor terminals due to the DAC (Digital to Analog Converter) offsets of the motion controller and the current sensor offsets of the current tracking amplifier. These current offsets generate sinusoidal torque disturbance and hence produce velocity ripples. Such a disturbance cannot be rejected by using a simple PI (Proportional plus Integral) control. Furthermore, the current offsets drift with time and temperature so that an off-line compensation does not work satisfactorily. In this paper, an optimal robust TDF (Two Degree of Freedom) regulator containing the internal model of the sinusoidal disturbance is proposed to accomplish disturbance rejection and constant speed tracking.*

Key words: Internal model principle, AC permanent magnet motor, velocity ripple elimination, current offsets, sinusoidal disturbance.

1 Introduction

Precision speed control systems are crucial in numerous industrial applications. For example, one typical application can be found in the feed control of machine tools in the manufacturing industry, where accurate smooth position and speed control are required for contour accuracy and small surface roughness of the products [1].

AC PM (Permanent Magnet) motors are attractive candidates for high performance industrial control applications such as the one stated above. In general, an AC PM control system consists of a motion controller, a current tracking amplifier, a feedback encoder and the motor itself. Fig. 1 shows the block diagram of a typical AC PM motor control system.

However, DC offsets are always present at the motor terminals due to the DAC (Digital to Analog Converter) offsets of the motion controller and current sensor offsets of the current tracking amplifier. These current offsets generate sinusoidal torque disturbance and hence produce velocity ripples. Such a disturbance cannot be rejected by using a simple PI (Proportional plus Integral) control. Furthermore, the current offsets drift with time and temperature so that an off-line compensation does not work satisfactorily. In [2], an adaptive scheme based on the Lyapunov function method was developed to estimate the amplitudes of the periodic disturbances and then use the amplitude information to minimize the torque ripples of an AC PM motor. In [5], another adaptive scheme was developed to first identify the amplitude and the phase of the periodic disturbance and then use this information to cancel the repetitive vibrations. In this paper, a simple but effective method, based on a TDF (Two Degree of Freedom) control structure and IMP (Internal Model Principle) [6], is employed to solve the problem of robust disturbance rejection and tracking without estimating the amplitude and the phase of the sinusoidal disturbance explicitly.

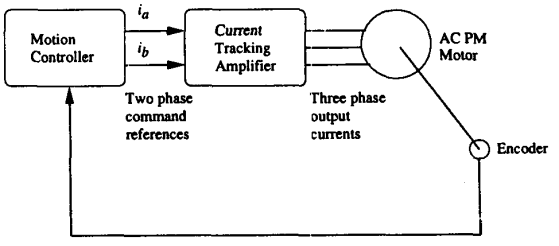

Figure 1: AC PM Motor Control System

The paper is organized as follows. Section 2 gives a brief review on the vector control of AC PM motors and the current offset disturbance modeling. In Section 3, the use of the IMP is proposed to solve the sinusoidal disturbance problem. Then a two stage TDF controller design procedure is given to achieve a desired tracking performance and reject the sinusoidal disturbance simultaneously. The LQR (Linear Quadratic Regulator) design methodology is em-

*This work is supported by Hong Kong Research Grants Council

ployed in the first stage to place the closed poles optimally and then a $\mathcal{H}_2$ norm optimization algorithm is proposed in the second stage to achieve a desired transient response. Section 4 presents the simulation results of the proposed method. In Section 5, experimental results are compared with the simulation results to validate our control methodologies. Some concluding remarks are given in Section 6.

2 Vector Control and Disturbance Modeling

A three phase AC PM motor can be modeled in $d-q$ frame by the following equations [7]:

$$v_d = R_s i_d + \frac{d(L_d i_d + \lambda_m)}{dt} - \omega_e L_q i_q \quad (1)$$

$$v_q = R_s i_q + \frac{d(L_q i_q)}{dt} + \omega_e (L_d i_d + \lambda_m) \quad (2)$$

$$\tau_e = \frac{3}{2}\frac{P}{2}[\lambda_m i_q - (L_q - L_d) i_d i_q] \quad (3)$$

$$\tau_e - \tau_l = J_m \frac{d\omega}{dt} + B_m \omega \quad (4)$$

where the parameters and variables have the following meanings:

R_s	stator winding resistance
P	number of poles (even number)
L_d, L_q	$d-q$ frame stator inductances
J_m	moment of inertia
B_m	friction constant
λ_m	constant magnetic flux
v_d, v_q	$d-q$ frame stator voltages
i_d, i_q	$d-q$ frame stator currents
τ_e	electro-mechanical torque
τ_l	load torque
ω	rotor mechanical speed
$\omega_e = \frac{P}{2}\omega$	rotor electrical speed.

If a sufficiently fast current tracking loop is used, (1) and (2) can be eliminated. In this case, i_d and i_q become the system inputs. Furthermore, the vector control technique suggests to set $i_d = 0$. This converts the nonlinear AC PM motor system into a linear system:

$$\tau_e = \frac{3}{2}\frac{P}{2}\lambda_m i_q \quad (5)$$

$$\tau_e - \tau_l = J_m \frac{d\omega}{dt} + B_m \omega \quad (6)$$

where λ_m is a constant magnetic flux.

When the motor current amplifier is connected to the power source and the two current reference commands from the motion controller are kept at zero, a DC offset current induced by current sensor offsets and the motion controller DAC offsets may be present in one or both of the closed loop controlled phases and thus also in the third one [4]. Let I_a, I_b be the two DC current offsets present at the motor terminals due to motion controller DAC offsets and the current amplifier sensor offsets. Then $I_c = -(I_a + I_b)$ is the third phase current offset. Let i_a^*, i_b^* and i_c^* be the desired currents at the motor terminals. By following the derivation in [3], when the three phase currents with offsets enter into the motor, the electro-mechanical torque for surface PM rotor type AC servo motors ($L_q = L_d$ [9]) can be decomposed into two parts as follows:

$$\tau_e = \tau_e^* + \tau_{off} \quad (7)$$

where

$$\tau_e^* = \frac{3}{2}\frac{P}{2}\lambda_m i_q^* \quad (8)$$

is the desired torque and i_q^* is the desired current which contains only i_a^*, i_b^* and i_c^*. The offset torque is equal to

$$\tau_{off} = \frac{P}{2}\lambda_m I_a \left[\frac{3}{2}\sin(\theta_e) - \frac{\sqrt{3}}{2}\cos(\theta_e)\right] - \frac{P}{2}\lambda_m I_b \left[\sqrt{3}\cos(\theta_e)\right] \quad (9)$$

where $\theta_e(t) = \theta_e(0) + \int_0^t \omega_e(t)dt$ is the electrical angle.

When the motor is performing a constant speed tracking with reference ω_r, $\omega_e(t)$ can be approximated, at least after certain transient period, by a constant $\omega_d = \frac{P}{2}\omega_r$. This shows that τ_{off} can be approximated by a sinusoidal function:

$$\tau_{off} = A_d \cos(\omega_d t - \phi_d) \quad (10)$$

where A_d is the magnitude of the disturbance while ϕ_d is the phase of the disturbance.

In summary, after employing the vector control algorithm and the formulation of the sinusoidal disturbance, the model of a vector controlled AC PM motor is given by Fig. 2. Here, $u = i_q^*$ is the input current, $y = \omega$ is the output velocity, $K_t = \frac{3}{2}\frac{P}{2}\lambda_m$ is the equivalent torque constant, τ_l is the load torque which can be considered as an unknown constant disturbance, τ_{off} is the torque disturbance due to current offsets which can be approximated by a sinusoidal function with known frequency ω_d and unknown magnitude and phase. Our goal is to design a good controller so that the output speed tracks a constant reference and rejects the disturbance τ_{off} and τ_l. Such a good controller is required to be robust, i.e. to perform the tracking and disturbance rejection even when the the system parameters vary slightly, to have good transient response, and to have a simple structure, i.e. to have an order as small as possible.

3 Controller Design

The problem to accomplish robust tracking and disturbance rejection is called a robust regulator problem. The key idea to solve a robust regulator problem is, based on the IMP, to have the controller to

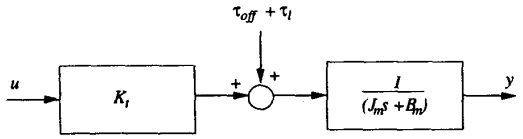

Figure 2: System Model with Disturbances

include the modes of the reference and disturbance. We also propose to use TDF controller structure to achieve better transient responses and easier designs. A TDF controller has a structure shown in Fig. 3. One of its advantages, in comparison with the usual one degree of freedom or unity feedback structure, is that the tracking performance depends only on K_1, and the robustness and the disturbance rejection performance depends only on K_2. Hence K_1 and K_2 can be independently designed with different consideration. We also give a simple yet systematic two stage optimization design procedure for the optimal robust TDF regulators which yields low order controllers.

3.1 Optimal Robust TDF Regulators and Two Stage Optimization Design

In Fig. 3, let G be a SISO (Single Input Single Output), first order and strictly proper plant described by the following transfer function:

$$G(s) = \frac{b(s)}{a(s)} \tag{11}$$

where $a(s) = s + a_1$ and $b(s) = b_1$. The TDF controller can be written as:

$$[\ K_1(s) \quad K_2(s)\ ] = \frac{1}{l(s)}[\ q(s) \quad h(s)\ ] \tag{12}$$

where

$$\begin{aligned} l(s) &= s^{n_l} + l_1 s^{n_l-1} + \cdots + l_{n_l} \\ q(s) &= q_0 s^{n_l} + q_1 s^{n_l-1} + \cdots + q_{n_l} \\ h(s) &= h_0 s^{n_l} + h_1 s^{n_l-1} + \cdots + h_{n_l}. \end{aligned} \tag{13}$$

With the above definitions, Fig. 3 can be converted into Fig. 4. The polynomials $l(s)$, $q(s)$ and $h(s)$ are designed in two stages. The first stage is to design $l(s)$ and $h(s)$ by using LQR methodology so that the closed loop poles are placed optimally. The second stage is to design $q(s)$ such that the overall transfer function $\frac{y(s)}{r(s)}$ can follow a desired system model.

In the first stage design, $l(s)$ and $h(s)$ are designed by using the state space equations. The SISO, first order and strictly proper plant G can be represented by the following state space equations:

$$\begin{aligned} \dot{x}(t) &= Ax(t) + Bu(t) + Ed(t) \\ y(t) &= Cx(t) \end{aligned} \tag{14}$$

where $A, B, C, E \in \mathbf{R}$, $u(t) \in \mathbf{R}$ is the input, $y(t) \in \mathbf{R}$ is the output which is to be regulated, $x(t) \in \mathbf{R}$ is the state which is linear proportional to the output in a first order system, $x(t) = C^{-1}y(t)$. $d(t) \in \mathbf{R}$ is the disturbance which is not measurable. It is assumed that the disturbance vector $d(t)$ satisfies the following equations:

$$d(t) = C_w z_w(t), \quad \dot{z}_w(t) = A_w z_w(t) \tag{15}$$

where $z_w(t) \in \mathbf{R}^{n_w}$, the pair (C_w, A_w) is observable. The reference signal $r(t)$ satisfies the following equations:

$$r(t) = C_r z_r(t), \quad \dot{z}_r(t) = A_r z_r(t) \tag{16}$$

where $z_r(t) \in \mathbf{R}^{n_r}$, the pair (C_r, A_r) is observable. We assume further that all the eigenvalues of A_w and A_r are in the closed right-half complex plane.

It is required to construct a controller for the system (14), using the available measurement $y(t)$ so that the resulting controlled system is stable and the error steady-state value is zero (i.e. asymptotic regulation takes place) for all disturbances $d(t)$ satisfying (15) and $r(t)$ satisfying (16).

Now we shall state the necessary and sufficient conditions for the existence of a solution to the problem of designed robust controllers for solving the servomechanism problem stated above.

Let the minimal polynomials of A_w and A_r be denoted by $m_w(s)$ and $m_r(s)$. Let $m(s)$ be the monic least common multiple of $m_w(s)$ and $m_r(s)$. Let

$$m(s) = s^{n_m} + m_1 s^{n_m-1} + \cdots + m_{n_m} = \prod_{i=1}^{n_m}(s - \lambda_i) \tag{17}$$

where λ_i, $i = 1, \cdots, n_m$, are the roots of $m(s)$. Then we define a controllable pair matrices (Ω, β) such that Ω has eigenvalues λ_i, $i = 1, \cdots, n_m$, and β is chosen to ensure that the matrix pair (Ω, β) is controllable.

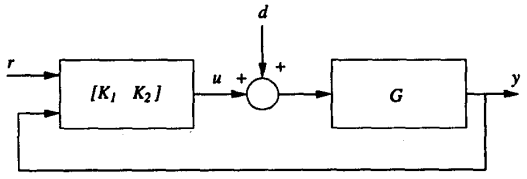

Figure 3: General TDF Controller Structure

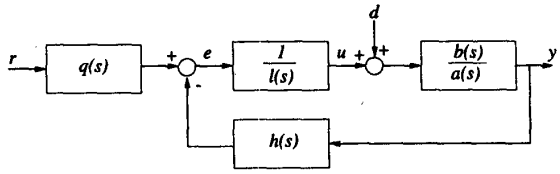

Figure 4: TDF Controller Structure

Theorem 3.1 *[10]A robust controller which solves the servo-mechanism problem stated above, can be found if and only if the following conditions are satisfied:*

1. (A, B) *is a stabilizable pair*
2. (C, A) *is a detectable pair*
3. $rank \begin{bmatrix} A - \lambda_i I & B \\ C & 0 \end{bmatrix} = 2,\ i = 1, 2, ..., n_m.$

When conditions (1)-(3) of the above theorem are satisfied, a robust controller can be designed using the available measurement $y(t)$, such that the resulting closed loop system is stable and asymptotic regulation takes place for all disturbance $d(t)$ and reference signal $r(t)$ defined by (15) and (16) respectively. Such a controller consists of a *servo-compensator*, which is completely determined by the disturbances and reference signals. A block diagram implementation of the robust controller is shown in Fig. 5 while the input reference signal $r(t)$ is ignored here. The robust controller satisfies the following equations :

$$u(t) = -k_1 x(t) - k_2 \xi(t) \tag{18}$$

where $\xi(t) \in \mathbf{R}^{n_m}$ is the output of the servo compensator defined by

$$\dot{\xi}(t) = \Omega \xi(t) + \beta y(t) \tag{19}$$

where β is chosen so that (Ω, β) is a controllable pair. In the present context, the stabilizing compensator and the matrices k_1 and k_2 are determined so that the augmented system consisting of the open loop system, together with the servo-compensator, is stabilized. In order to get the equations of the augmented system, let us write the system equations, together with the servo compensator equations, as follows:

$$\begin{aligned} \underbrace{\begin{bmatrix} \dot{x} \\ \dot{\xi} \end{bmatrix}}_{\dot{\hat{x}}} &= \underbrace{\begin{bmatrix} A & 0 \\ \beta C & \Omega \end{bmatrix}}_{\hat{A}} \underbrace{\begin{bmatrix} x \\ \xi \end{bmatrix}}_{\hat{x}} + \underbrace{\begin{bmatrix} B \\ 0 \end{bmatrix}}_{\hat{B}} u \\ &\quad + \begin{bmatrix} E \\ \beta F \end{bmatrix} d \\ y &= \begin{bmatrix} C & 0 \end{bmatrix} \begin{bmatrix} x \\ \xi \end{bmatrix}. \end{aligned} \tag{20}$$

The matrices k_1 and k_2 can now be designed to stabilize the augmented system $\dot{\hat{x}} = \hat{A}\hat{x} + \hat{B}u$. Since (A, B) is a stabilizable pair (by existence condition (1) of Theorem 3.1) and (Ω, β) is a controllable pair (by choice of β), it follows that the system (14) is stabilizable by means of state feedback. The LQR design methodology is employed here for the designs of k_1 and k_2 such that the cost function

$$J = \int_0^\infty (\hat{x}' Q \hat{x} + u' R u) dt \tag{21}$$

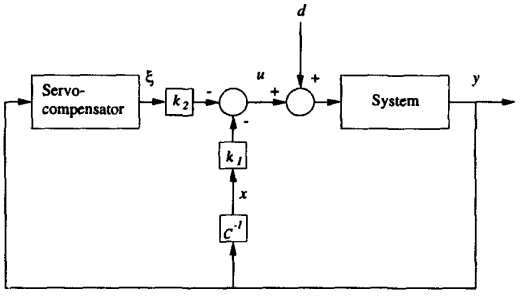

Figure 5: First Stage Controller Design (reference signal r is ignored)

is minimized by a proper choice of matrices Q and R. k_1 and k_2 can be found by first solving the solution, S, of the following Riccati equation:

$$S\hat{A} + \hat{A}'S - S\hat{B}R^{-1}\hat{B}'S + Q = 0, \tag{22}$$

then

$$\begin{bmatrix} k_1 & k_2 \end{bmatrix}' = R^{-1} S \hat{B}. \tag{23}$$

After k_1 and k_2 are found, the polynomials $h(s)$ and $l(s)$ can be evaluated since $\frac{u}{y} = \frac{h(s)}{l(s)}$ is the transfer function realization of the following state space equations:

$$\frac{h(s)}{l(s)} = k_2 (sI - \Omega)^{-1} \beta + C^{-1} k_1 \tag{24}$$

where

$$\begin{aligned} n_l &= n_m \\ l(s) &= s^{n_l} + l_1 s^{n_l - 1} + \cdots + l_{n_l} \\ &= s^{n_m} + m_1 s^{n_m - 1} + \cdots + m_{n_m} \\ h(s) &= h_0 s^{n_l} + h_1 s^{n_l - 1} + \cdots + h_{n_l}. \end{aligned}$$

Without loss of generality, $h(s)$ will be put in the feedback path and $\frac{1}{l(s)}$ will be put in the forward path in the actual implementation as shown in Fig. 4.

The second stage is to design the polynomial $q(s)$ so that the overall transfer function can follow a desired model. In reference to Fig. 4, the closed loop transfer function can be written as:

$$\frac{y(s)}{r(s)} = \frac{q(s)b(s)}{l(s)a(s) + h(s)b(s)} := \frac{q(s)b(s)}{\delta(s)} \tag{25}$$

where

$$\delta(s) = s^{n_l + 1} + \delta_1 s^{n_l} + \cdots + \delta_{n_l + 1}.$$

To achieve a robust tracking performance, it requires

$$q(s) = h(s) - f(s) m_r(s) \tag{26}$$

where $f(s) = f_0 s^{n_f} + f_1 s^{n_f - 1} + \cdots + f_{n_f}$ is a polynomial to be designed, $n_f = n_l - \deg m_r(s)$ and $m_r(s)$ is a monic polynomial contains the unstable modes of r. Finally, we would like our overall transfer function

$\frac{y(s)}{r(s)}$ to follow a desired model $G_m(s)$; therefore, $f(s)$ is designed to minimize the following $\mathcal{H}_2$ norm:

$$\|\tilde{G}(s)\|_2 := \left\| \left\{ G_m(s) - \frac{[h(s) - f(s)m_r(s)]b(s)}{l(s)a(s) + h(s)b(s)} \right\} \frac{1}{m_r(s)} \right\|_2 \quad (27)$$

where $G_m(s)$ is a desired model such as a first order low pass system. Let the minimal controllable state space realization of the above transfer function be

$$\tilde{G}(s) = \tilde{C}(sI - \tilde{A})^{-1}\tilde{B}, \quad (28)$$

where the $(\tilde{A}, \tilde{B})$ pair is in controllable canonical form, $\tilde{C} = \bar{C}_0 + \bar{f}\bar{C}_1$ and $\bar{f} = [\ f_0 \quad f_1 \quad \cdots \quad f_{n_f}\ ]$. The $\mathcal{H}_2$ norm of system $\tilde{G}$ can be found by following the approach in [12],

$$\|\tilde{G}(s)\|_2^2 = \mathrm{tr}(\tilde{C}\tilde{P}\tilde{C}') \quad (29)$$

and $\tilde{P}$ is the controllability Gramian that can be obtained from the Lyapunov equation, $\tilde{A}\tilde{P} + \tilde{P}\tilde{A}' + \tilde{B}\tilde{B}' = 0$. For a SISO system,

$$\mathrm{tr}(\tilde{C}\tilde{P}\tilde{C}') = \tilde{C}\tilde{P}\tilde{C}' = \tilde{C}\tilde{P}^{\frac{1}{2}}\tilde{P}^{\frac{1}{2}}\tilde{C}' \quad (30)$$

and

$$\tilde{C}P^{\frac{1}{2}} = \underbrace{\bar{C}_0 P^{\frac{1}{2}}}_{\bar{b}} + \bar{f}\underbrace{\bar{C}_1 P^{\frac{1}{2}}}_{\bar{A}}. \quad (31)$$

Therefore, the above minimization problem is now equal to minimize the following $\mathcal{H}_2$ norm:

$$\|\bar{f}\bar{A} + \bar{b}\|_2. \quad (32)$$

Then $\bar{f}$ can be easily found by the following equation [13]:

$$\bar{f} = -\bar{b}\bar{A}'(\bar{A}\bar{A}')^{-1} \quad (33)$$

3.2 Design for the PM Motor Control System

For our PM motor control system, in reference to Fig. 4, we have $a(s) = s + \frac{B_m}{J_m}$ and $b(s) = \frac{K_t}{J_m}$. The state space equations of the PM motor control system can be found in (14) with the parameters $A = -\frac{B_m}{J_m}$, $B = 1$, $C = \frac{K_t}{J_m}$ and $E = \frac{1}{K_t}$. Since r is a step reference, it follows that $m_r(s) = s$. Since d contains a sinusoidal function of frequency $\omega_d = \frac{P}{2}\omega_r$ and a constant function, it follows that $m_w(s) = s(s^2 + \omega_d^2)$. Therefore, $m(s) = s(s^2 + \omega_d^2)$. The matrix Ω is chosen to be

$$\Omega = \begin{bmatrix} 0 & 1 & 0 \\ 0 & 0 & 1 \\ 0 & -\omega_d^2 & 0 \end{bmatrix}, \quad (34)$$

and its eigenvalues are equal to $\lambda_1 = 0$, $\lambda_2 = -j\omega_d$ and $\lambda_3 = j\omega_d$. Here, $\beta = [\ 0 \quad 0 \quad 1\ ]'$ is chosen such that (Ω, β) is a controllable pair. Now $(A, B) = (-\frac{B_m}{J_m}, 1)$ and $(C, A) = (\frac{K_t}{J_m}, -\frac{B_m}{J_m})$ are stabilizable and detectable pairs respectively. Furthermore,

$$\mathrm{rank}\begin{bmatrix} -\frac{B_m}{J_m} - \lambda_i & 1 \\ \frac{K_t}{J_m} & 0 \end{bmatrix} = 2$$

for $i = 1, 2, 3$. It concludes that our problem is solvable by Theorem 3.1. It follows that the matrices $\hat{A}$ and $\hat{B}$ defined in (20) are equal to

$$\hat{A} = \begin{bmatrix} -\frac{B_m}{J_m} & 0 & 0 & 0 \\ 0 & 0 & 1 & 0 \\ 0 & 0 & 0 & 1 \\ \frac{K_t}{J_m} & 0 & -\omega_d^2 & 0 \end{bmatrix} \quad (35)$$

and

$$\hat{B} = [\ 1 \quad 0 \quad 0 \quad 0\ ]'. \quad (36)$$

Now we can choose the matrices R and Q to place our closed loop poles by optimizing the function defined in (21). As suggested by [11], for a single input system, one can choose $R = 1$ and $Q = \rho ww'$ with the zeros of $w'(sI - \hat{A})^{-1}\hat{B}$ coinciding with $(n-1)$ closed loop poles. Then one can choose ρ to move the remaining closed loop pole towards infinity. The smaller ρ is, the less accurate will be the pole positioning. After designing k_1 and k_2 by solving (22) and (23), the polynomials $h(s)$ and $l(s)$ can be found by the following equations:

$$\frac{h(s)}{l(s)} = k_2(sI - \Omega)^{-1}\beta + k_1\frac{J_m}{K_t} \quad (37)$$

where $l(s) = s^3 + \omega_d^2 s$ and $h(s) = h_0 s^3 + h_1 s^2 + h_2 s + h_3$.

By following the design procedure in Section 3.1, the second stage is to design the polynomial $q(s)$ defined in (25) such that the $\mathcal{H}_2$ norm in (27) can be optimized. Since $m_r(s) = s$ in our application, it follows that $f(s) = f_0 s^2 + f_1 s + f_2$ in (26). Consequently, the final step is to design $f(s)$ so that the overall transfer function from r to y can follow a desired model $G_m(s)$. The first order system $G_m(s) = \frac{1}{Ts+1}$ is chosen to be the desired model and from (28),

$$\tilde{A} = \begin{bmatrix} -(\delta_1 + \frac{1}{T}) & -(\delta_2 + \frac{\delta_1}{T}) & -(\delta_3 + \frac{\delta_2}{T}) & -(\delta_4 + \frac{\delta_3}{T}) & -\frac{\delta_4}{T} \\ 1 & 0 & 0 & 0 & 0 \\ 0 & 1 & 0 & 0 & 0 \\ 0 & 0 & 1 & 0 & 0 \\ 0 & 0 & 0 & 1 & 0 \end{bmatrix},$$

$$\tilde{B} = [\ 1 \quad 0 \quad 0 \quad 0 \quad 0\ ]' \quad (38)$$

and

$$\tilde{C} = [0 \quad \tfrac{1}{T} - h_0\tfrac{K_t}{J_m} \quad \tfrac{B_m}{J_m T} - h_1\tfrac{K_t}{J_m} \quad \tfrac{\omega_d^2}{T} - h_2\tfrac{K_t}{J_m} \quad \tfrac{B_m\omega_d^2}{J_m T} - h_3\tfrac{K_t}{J_m}] + [\ f_0 \quad f_1 \quad f_2\ ] \begin{bmatrix} 0 & \frac{K_t}{J_m} & \frac{K_t}{J_m T} & 0 & 0 \\ 0 & 0 & \frac{K_t}{J_m} & \frac{K_t}{J_m T} & 0 \\ 0 & 0 & 0 & \frac{K_t}{J_m} & \frac{K_t}{J_m T} \end{bmatrix}$$

$$:= \bar{C}_0 + \bar{f}\bar{C}_1 \quad (39)$$

where $\bar{f} = [\ f_0 \quad f_1 \quad f_2\ ]$. Finally, $\bar{f}$ can be found in (33).

4 Simulation Results

A 200W AC PM motor is used in our simulations and experimental tests. The motor parameter is listed in Table 1.

To show our controller effectiveness, a traditional PI controller is always used for comparison. In addition, a -0.1A current offset is assumed presenting at phase 1 of the motor terminal and a 0.05A current offset is assumed presenting at phase 2 of the motor terminal.

4.1 Simulation Results for the Optimal Robust TDF Regulator

Assume that the reference speed is $\omega_r = 100$ rpm $= 10.472$ rad·s^{-1}. Then $\omega_d = \frac{8}{2} \times \omega_r = 41.88$ rad·s^{-1}. $R = 1$ and $Q = \rho w w'$, where $\rho = 100$ and

$$w = [\ 1 \quad 1000 \quad 100 \quad 1\ ],$$

are chosen. After solving (22) and (23), $k_1 = 536.7456$ and

$$k_2 = [10^4\ 955.9113\ 13.9239]$$

can be found. The four closed loop poles are located at $-2.37\times10^2 \pm j2.47\times10^2$, -89.42 and -11.25. Now $l(s)$ and $h(s)$ defined in (37) can be evaluated as

$$\begin{aligned} l(s) &= s^3 + 1754.6s \\ h(s) &= 0.0457s^3 + 13.9239s^2 + 1036.1s + 10000. \end{aligned}$$

The next step is to design the polynomial $q(s)$ so that our overall transfer function can follow a desired model $G_m(s) = \frac{1}{0.01s+1}$. By following the design procedure proposed in the previous section, we get

$$\begin{aligned} f(s) &= 0.0384s^2 + 9.5331s + 92.6318 \\ q(s) &= h(s) - f(s)m_r(s) \\ &= 0.0073s^3 + 4.3908s^2 + 943.4261s + 10000 \end{aligned}$$

and the three zeros of the overall system are located at $-2.95\times10^2 \pm j1.98\times10^2$ and -11.17.

Table 1: Motor Parameter

J_m	0.144×10^{-4}kg·m^2
B_m	5.416×10^{-4}Nm/rad·s^{-1}
λ_m	0.0283Wb
L_d	11.5mH
L_q	11.5mH
P	8
$K_t = \frac{3}{2}\frac{P}{2}\lambda_m$	0.1698Nm/A
Encoder resolution	8000 counts/rev

Fig. 6 shows the simulation results comparison between the proposed optimal robust TDF regulator and a PI controller with $k_p = 0.01$ and $k_i = 0.08$. It can be observed that the velocity ripples due to DC current offset can be rejected by the proposed controller completely in steady state.

In summary, the optimal robust TDF regulator can reject the sinusoidal disturbance with guaranteed output tracking response. On the contrary, a PI speed controller fails to reject the sinusoidal disturbance. This is expected since the PI controller doesn't contain all modes of the disturbance.

5 Experimental Results

Experiments are performed to verify the effectiveness of our proposed controllers. Fig. 1 shows the basic setup of our experiment. A dSAPCE DS1102 DSP controller board is used as our motion controller. In connection with MATLAB real time workshop and SIMULINK, a fast prototyping working environment is achieved and hence the code development time can be saved. The DSP controller implements all control algorithms with a sampling frequency 2kHz. In every control cycle, the controller reads the motor encoder, performs the control algorithm calculation and then outputs two current reference commands i_a and i_b to the current tracking amplifier. An Advanced Motion Controls Inc. S30A40B current tracking driver is used and the three phase AC PM motor is from Sanyo Denki with the parameters listed in Table 1.

An experiment is conducted with command reference speed equal to 0.4 Hz square waves with amplitude 100 rpm $= 10.472$ rad·s^{-1}. The controller is the same as in Section 4. Fig. 7 shows the velocity output when only a PI controller with $k_p = 0.01$ and $k_i = 0.08$ is used. It is clear that the output velocity contains ripples with the peak value equals to 30% of the command value. Fig. 8 shows the velocity output when the optimal robust TDF regulator is used. The velocity output ripples are reduced to the mo-

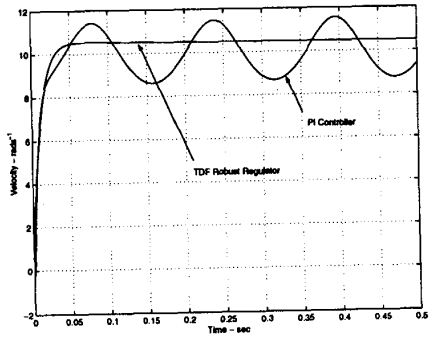

Figure 6: Simulation Results Comparison between the Optimal Robust TDF Regulator and the PI Controller, $\omega_r = 100$ rpm

tor encoder resolution, which is, the best we can do. In our system, the motor encoder resolution is equal to 8000 counts/rev and our servo loop sampling frequency is 2kHz; therefore, the smallest velocity ripples are equal to $\frac{2000\times2\times\pi}{8000} = 1.5708$ rad·s^{-1}. The output velocity ripples are believed to be further reduced if a higher resolution encoder is used.

Our experimental results match well with the simulation results in the last section. They validate that the controller proposed in Section 3 can reject the sinusoidal disturbance and achieve a desired output tracking performance at the same time.

6 Conclusions

In this paper, the optimal robust TDF regulator for AC PM motors based on the IMP is demonstrated to be an effective method to eliminate the velocity ripples that are created by DC current offsets. Furthermore, by following our proposed systematic optimal robust TDF regulator design method, both the velocity tracking and the disturbance rejection requirement can be achieved simultaneously. A velocity ripple-free output is crucial to some constant speed requirement applications such as machine feed control and assembly line application, etc.

Notice that the controller design in Section 3 depends on the reference speed, ω_r. In some application which requires variable speed reference, the adaptive version of the proposed controller for online adjustment in response to the change in speed reference is required. We are now working on this direction so that an adaptive controller can be developed for varying speed references.

References

[1] Y. Liu and D. Chen, "Adaptive Rejection of Velocity-Ripple From Position Transducer In A Motion Control System," Proc. of the 33rd Conference on Decision and Control, pp. 690-695, 1994.

[2] V. Petrovic, R. Ortega, A. M. Stankovic and G. Tadmor, "An Adaptive Controller for Minimization of Torque Ripple in PM Synchronous Motors," PESC 98 Record. 29th Annual IEEE Power Electronics Specialists Conference, vol. 1, pp.113-118, 1998.

[3] W. C. Gan and L. Qiu, "Robust Two Degree of Freedom Regulator for Velocity Ripple Elimination of AC Permanent Magnet Motors," submitted to IEEE International Conference on Control Applications, 2000

[4] G. Ferretti, G. Magnani and P. Rocco, "Modeling, Identification, and Compensation of Pulsating Torque in Permanent Magnet AC Motors," IEEE Trans. Industrial Electronics, vol. 45, no. 6, pp. 912-920, Apr. 1998.

[5] M. Bodson, "A Discussion of Chaplin and Smith's Patent for the Cancellation of Repetitive Vibrations," IEEE Trans. Automatic Control, vol. 44, no. 11, pp. 2221-2225, Nov. 1999.

[6] B. Francis, O. A. Sebakhy and M. W. Wohham, "Synthesis of multivariable regulators: the internal model principle", Appl. Math. Optimiz., vol 1, pp. 64-86, 1974.

[7] D. W. Novotny and T. A. Lipo, Vector Control and Dynamics of AC Drives, Oxford, 1998.

[8] M. Vidyasagar, Control System synthesis, The MIT Press, Cambridge, 1985.

[9] I. Boldea and S. A. Nasar, Electric Drives, CRC Press, 1999.

[10] R. V. Patel and N. Munro, Multivariable System Theory and Design, Pergamon Press, 1982.

[11] B. D. O. Anderson and J. B. Moore, Optimal Control Linear Quadratic Methods, Prentice Hall, 1990.

[12] K. Zhou and J. C. Doyle, Essentials of Robust Control, Prentice Hall, 1998.

[13] G. H. Golub and C. F. V. Loan, Matrix Computations, Johns Hopkins, 1996.

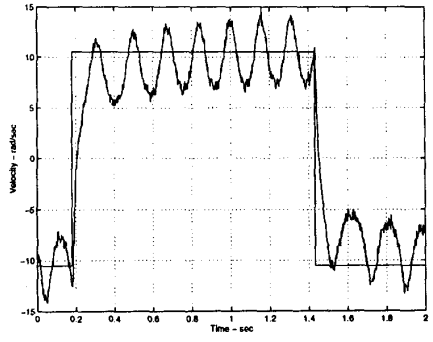

Figure 7: Experimental Velocity Output - PI Controller, $\omega_r = 100$ rpm

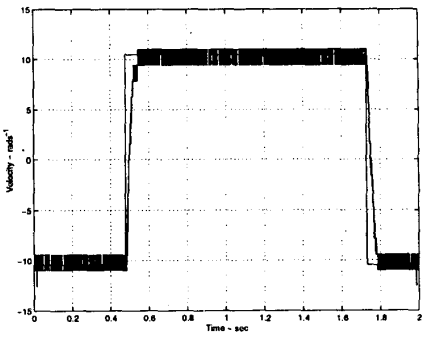

Figure 8: Experimental Velocity Output - Optimal Robust TDF regulator, $\omega_r = 100$ rpm